$NaCrO_2$/Coffee Waste–derived Nitrogen-doped Carbon Composite as High-Performance Cathode Material for Sodium Ion Batteries

Seok Mun Kang,[†,‡] Min-Seob Kim,[†,‡] Yunseo Jeoun,[†,‡] Chairul Hudaya,[§] and Yung-Eun Sung[†,‡,*]

[†]*Center for Nanoparticle Research, Institute for Basic Science (IBS), Seoul 08826, Republic of Korea*
[‡]*School of Chemical & Biological Engineering, Seoul National University, Seoul 08826, Republic of Korea. *E-mail: ysung@snu.ac.kr*
[§]*Department of Electrical Engineering, Faculty of Engineering, Universitas Indonesia, Kampus Baru UI, Depok 16424, Indonesia*

Received April 17, 2019, Accepted June 14, 2019, Published online July 9, 2019

Sodium-ion batteries (NIBs) are promising alternatives to lithium-ion batteries for large-scale energy applications such as energy storage systems, owing to the earth-abundance and low cost of sodium resources. Among layered oxide cathode materials for NIBs, O3-type $NaCrO_2$ has attracted considerable attention owing to its electrochemically active $Cr^{3+/4+}$, which is unlike that of $LiCrO_2$, and potential for carbon coating with a high thermal stability. In this study, we propose a new facile and eco-friendly method for applying nitrogen-doped carbon to $NaCrO_2$ using coffee waste as a carbon source. The synthesized O3-type $NaCrO_2$/coffee waste–derived N-doped carbon composite exhibits an outstanding electrochemical performance as an NIB cathode material. The sodium/composite cell achieved a 73.7% capacity retention after 500 charge/discharge cycles and an approximate 50% discharge capacity during 43 s of charge. The results demonstrate the potential use of coffee waste for battery materials with improved electrochemical performances.

Keywords: Sodium ion battery, Coffee waste, Nitrogen-doped carbon, High-power cathode

Introduction

Since their commercialization in 1991, lithium ion batteries (LIBs) have been one of the most dominant power sources for various technologies, from portable electronics to large-scale applications such as electric vehicles and energy storage systems.[1–3] However, the main drawbacks of LIBs are the limited nature of lithium reserves and corresponding lithium price, which hinders their expansion to large-scale markets.[4,5] In this regard, sodium-ion batteries (NIBs) have attracted considerable attention as promising alternatives to LIBs because sodium is both more abundant and less expensive than lithium.[6–8] Moreover, NIBs share similar chemistry with LIBs, and thus the tremendous technological advancements of LIBs have also led to the rapid development of NIB technologies.

Na_xMO_2 (M = Mn, Fe, Co, Ni, etc.) compounds with layered structures are promising candidates as NIB cathode materials owing to their high energy densities and long cycle lives.[9–11] O3-type $NaCrO_2$ is a layered cathode compound employed in NIBs that can utilize the redox activity of $Cr^{3+/4+}$, unlike the electrochemically inactive $LiCrO_2$ used in LIBs.[12] The reversible specific capacity of $NaCrO_2$ is limited to approximately 110 mAh/g, which corresponds to approximately 0.5 Na^+ utilization per formula unit because further Na^+ extraction (Na_xCrO_2, $x < 0.4$) leads to a layered-to-rock-salt formation process with irreversible capacity losses.[13,14] Nonetheless, the flat charge/discharge profile (approximately 3 V *vs.* Na/Na^+), stable cycle life, and potential for carbon coating with a high thermal stability make the material attractive for use as NIB cathode electrodes.[15–17]

Previous studies have reported on the electrochemical performance improvement of $NaCrO_2$ by carbon coating.[16,17] Ding *et al*. fabricated carbon-coated $NaCrO_2$ particles using citric acid via a simple solid-state synthesis, which led to an increased cycle stability.[16] Yu *et al*. introduced new synthetic routes that included an emulsion-drying method for synthesizing $NaCrO_2$ and subsequent additional heat treatment using pitch as a carbon source for carbon coating.[17] The carbon-coated $NaCrO_2$ reported by Yu *et al*. exhibited an outstanding electrochemical performance with regards to cycle stability and rate capability. Inspired by the success of carbon-coated $NaCrO_2$, we decided to propose an efficient, simple, and inexpensive preparation method for carbon-coated $NaCrO_2$ without compromising the performance achieved by existing methods.

In this work, we report an O3-type $NaCrO_2$/coffee waste (CW)–derived N-doped carbon composite electrode material (denoted as NC–$NaCrO_2$) that can be used as a cathode material for NIBs. CW, or used coffee grounds, is an economically and environmentally friendly nitrogen-containing carbon source that should be utilized and recycled owing to

the large-scale worldwide production of coffee beans.[18] Therefore, various attempts have been made to utilize CW as a material source for energy applications including supercapacitors and dye-sensitized solar cells.[19,20] To take advantage of the nitrogen-doped carbon from CW, we introduced additional mixing of $NaCrO_2$ powder with CW followed by carbonization to produce a composite electrode material. We performed quantitative and qualitative analyses of the CW-derived N-doped carbon on the $NaCrO_2$ particle surfaces using thermogravimetric (TG) analysis, elemental analysis (EA), and transmission electron microscopy (TEM). We confirmed the outstanding electrochemical performance of NC–$NaCrO_2$ in terms of cycle stability and rate capability compared with bare $NaCrO_2$. The results indicate that the introduction of an N-doped carbon layer from CW is a highly economical and eco-friendly approach to improve the electrochemical properties of $NaCrO_2$.

Experimental

Material Syntheses. The O3-type $NaCrO_2$ powder was synthesized by a simple solid-state reaction. Using a ball-mill, Na_2CO_3 (Kanto Chemical, Tokyo, Japan) and Cr_2O_3 (Sigma-Aldrich, St. Louis, MO, USA) powders with a 1.02:1 M ratio were thoroughly mixed in an acetone medium. An excess 2 wt % of the sodium source was added to compensate for sodium loss during heat treatment owing to its high volatility. The homogenously mixed powders were heated under argon flow at 900 °C for 6 h. To synthesize the NC–$NaCrO_2$ composite, $NaCrO_2$ powder was mixed with fully dried CW extracted from capsule coffee by high energy ball-milling at 300 rpm for 30 min in an anhydrous *N*-methylpyrrolidone (Sigma-Aldrich) medium, in which the weight of the CW corresponded to 15 wt % of the $NaCrO_2$ powder. After drying under vacuum, the mixed powder was heated under argon flow at 800 °C for 2 h. The composite powder was then transferred to an argon-filled glove box as soon as possible to avoid unfavorable reactions with the ambient atmosphere and moisture.

Characterization. X-ray diffraction (XRD) patterns of sample powders were obtained using a Smartlab (Rigaku, Tokyo, Japan) diffractometer with Cu Kα radiation (1.5406 Å). Field emission scanning electron microscopy (FE-SEM) and TEM images for each sample were obtained using the MERLIN Compact (Zeiss, Oberkochen, Germany) and Tecnai F20 (FEI, Hillsboro, OR, USA) systems, respectively. TG analysis was conducted using an SDT Q600 (TA Instruments, New Castle, DE, USA), and EA was performed to obtain the C/H/N/S composition of the CW-derived carbon using a Flash 1112 (Thermo Fisher Scientific, Waltham, MA, USA).

Electrochemistry. Slurries of $NaCrO_2$ and NC–$NaCrO_2$ were prepared by mixing active material powders, Super P, and poly vinylidene fluoride in *N*-methylpyrrolidone with a weight ratio of 8:1:1 using a mortar and pestle. These homogeneously mixed slurries were cast onto Al foils and dried at 120 °C for 8 h under vacuum. The dried foils were roll-pressed before being used as cathodes. For the electrochemical tests, CR2032-type coin cells were assembled in an argon-filled glove box. Sodium metal (Sigma-Aldrich) was used as the anode, and 1 M $NaPF_6$ in ethylene carbonate/dimethyl carbonate (1:1 v/v) with 2 wt % fluoroethylene carbonate as an additive was used as the electrolyte. A glass fiber (Whatman GF-C) was used as a separator. Galvanostatic charge/discharge tests were performed using a WBCS3000S (WonAtech, Seoul, Korea) at 25 °C, and electrochemical impedance spectroscopy (EIS) was performed using an IM6 (ZAHNER-elektrik, Kronach, Germany).

Results and Discussion

As shown in Figure S1 (Supporting Information), the CW collected from spent coffee capsules consisted of dark brown, chopped pieces of coffee. Following heat treatment, the color of the $NaCrO_2$ powder mixed with dried CW clearly changed from bright to dark green owing to the presence of carbon on the powder surface (Figure 1(a)). The crystal structure of the O3-type layered $NaCrO_2$ along the c-axis is presented in Figure 1(b) and XRD patterns of the samples are presented in Figure 1(c). The major diffraction peaks of pristine $NaCrO_2$ are well matched with the reflection peaks of the $NaCrO_2$ reference (PDF# 25-0819). Pattern indexing confirmed the $NaCrO_2$ space group of R3m with lattice parameters a and c of 2.9752 (**2**) and 15.964 (**1**) Å, respectively. Additionally, in the XRD pattern of NC–$NaCrO_2$, no additional impurities were found from the formation of a composite with the CW-derived carbon. The lattice parameter values for NC–$NaCrO_2$ remained almost the same as those of the bare $NaCrO_2$ after ball-milling and heat treatment (Table S1).

Changes in the morphologies and particle sizes of each sample were observed by FE-SEM (Figure 2(a) and (b)). As shown in Figure 2(a), pristine $NaCrO_2$ exhibited a randomly grown form of hexagonal plate-like particles; the particle sizes were irregularly distributed with a minimum size of 500 nm. After additional ball-milling with CW and heat treatment, the particle sizes of NC-$NaCrO_2$ decreased, and particles of less than 500 nm appeared (Figure 2(b)). In the TEM images, a carbon layer with a thickness of approximately 20 nm from CW carbonization could clearly be observed at the NC–$NaCrO_2$ surface compared to bare $NaCrO_2$ (Figure 2(c) and (d)). At a lower magnification, bulk carbon can also be observed on some NC–$NaCrO_2$ particle surfaces (Figure S2).

To quantify the amount of CW-derived carbon, TG analysis was conducted for each sample. $NaCrO_2$ reacts with oxygen to produce Na_2CrO_4 and Cr_2O_3 at approximately 300–700 °C as given by:

$$NaCrO_2 + (3/8)O_2 \rightarrow (1/2)Na_2CrO_4 + (1/4)Cr_2O_3$$

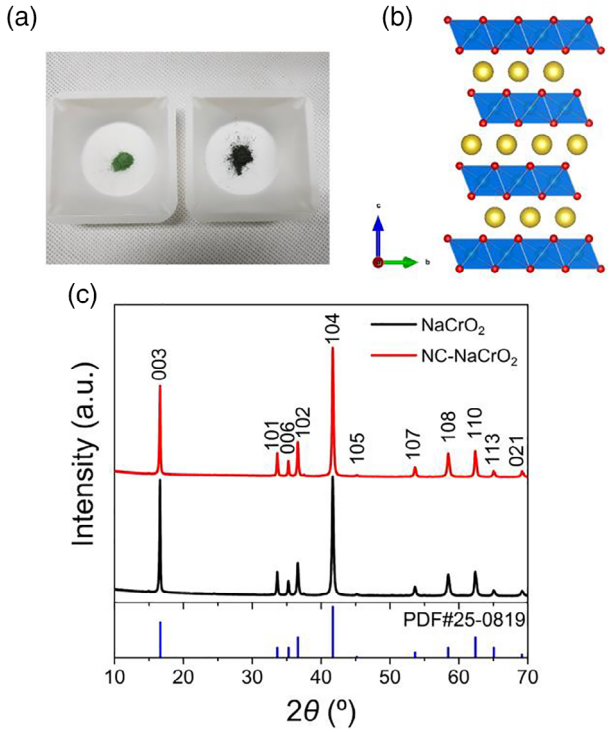

Figure 1. (a) Photograph of $NaCrO_2$ (left) and NC–$NaCrO_2$ (right) powders. (b) Schematic of layer-structured O3-type $NaCrO_2$ along the c-axis (yellow: Na, red: O, and blue: Cr). (c) XRD patterns of the $NaCrO_2$ and NC–$NaCrO_2$ powder samples.

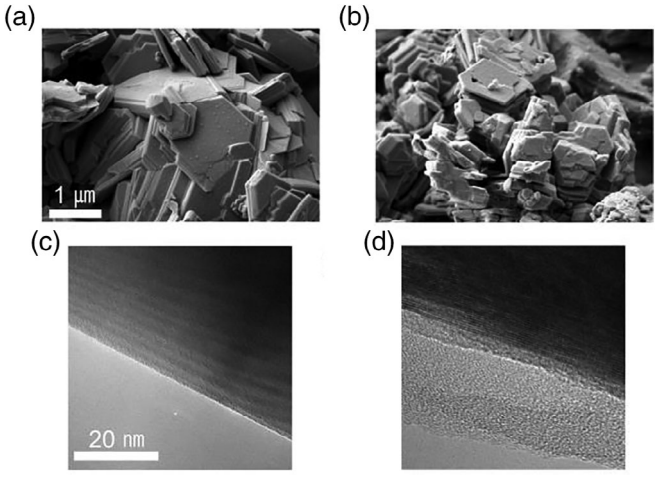

Figure 2. FE-SEM images of (a) $NaCrO_2$ and (b) NC–$NaCrO_2$ powder samples. TEM images of (c) $NaCrO_2$ and (d) NC–$NaCrO_2$ particle surfaces.

with a theoretical increase of 11.22 wt %. As determined by TG analysis, upon heating from 100 to 700 °C, the weights of $NaCrO_2$ and NC–$NaCrO_2$ increased by 10.54 and 7.346 wt %, respectively, as shown in Figure 3 (a) and (b). Assuming that the weight difference between NC–$NaCrO_2$ and $NaCrO_2$ is from the CW-derived carbon, the calculated amount of carbon is 2.89 wt %. This corresponds to a yield of approximately 20%, which is consistent with

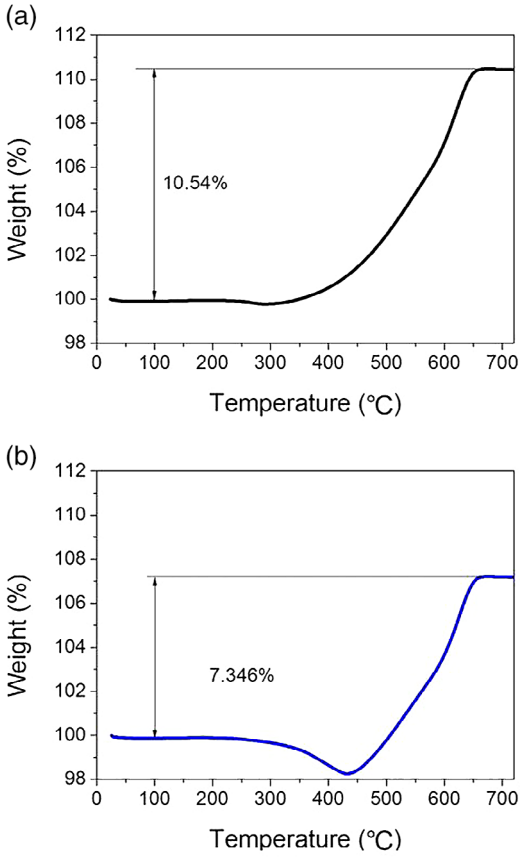

Figure 3. TG analysis curves of (a) $NaCrO_2$ and (b) NC–$NaCrO_2$ powders measured with a linear ramp of 10 °C/min in an air atmosphere.

previous reports.[20] CW-derived carbon generally has a nitrogen-doped form owing to its protein and caffeine residuals. The N/C ratio was confirmed for CW-derived carbon without $NaCrO_2$ to be approximately 4.50 wt % by EA as shown in Table S2.

Electrochemical cycling performance tests were performed for Na/$NaCrO_2$ and Na/NC–$NaCrO_2$ cells with a 2.0–3.6 V *vs.* Na/Na^+ cut-off condition and a current density of 100 mA/g (0.83C, 1C = 120 mAh/g) during 500 cycles. As shown in Figure 4(a), the first discharge capacities of $NaCrO_2$ and NC–$NaCrO_2$ were 117.7 and 116.3 mAh/g, respectively. NC–$NaCrO_2$ showed slightly lower discharge capacities than $NaCrO_2$, owing to the reduction of the active material by carbon addition. The first Coulombic efficiencies were 97.7% and 98.0% for $NaCrO_2$ and NC–$NaCrO_2$, respectively. In both cells after the first few charge/discharge cycles, Coulombic efficiencies greater than 99% were maintained. After 500 charge/discharge cycles, the discharge capacities of $NaCrO_2$, and NC–$NaCrO_2$ decreased to 69.3 and 85.7 mAh/g, which correspond to 58.9% and 73.7% capacity retentions, respectively. The charge/discharge profiles of the Na/$NaCrO_2$ and Na/NC–$NaCrO_2$ cells for the 1st, 50th, 100th, 200th, 300th, and 500th cycles are presented in Figure 4(b) and (c), respectively. In both samples, the

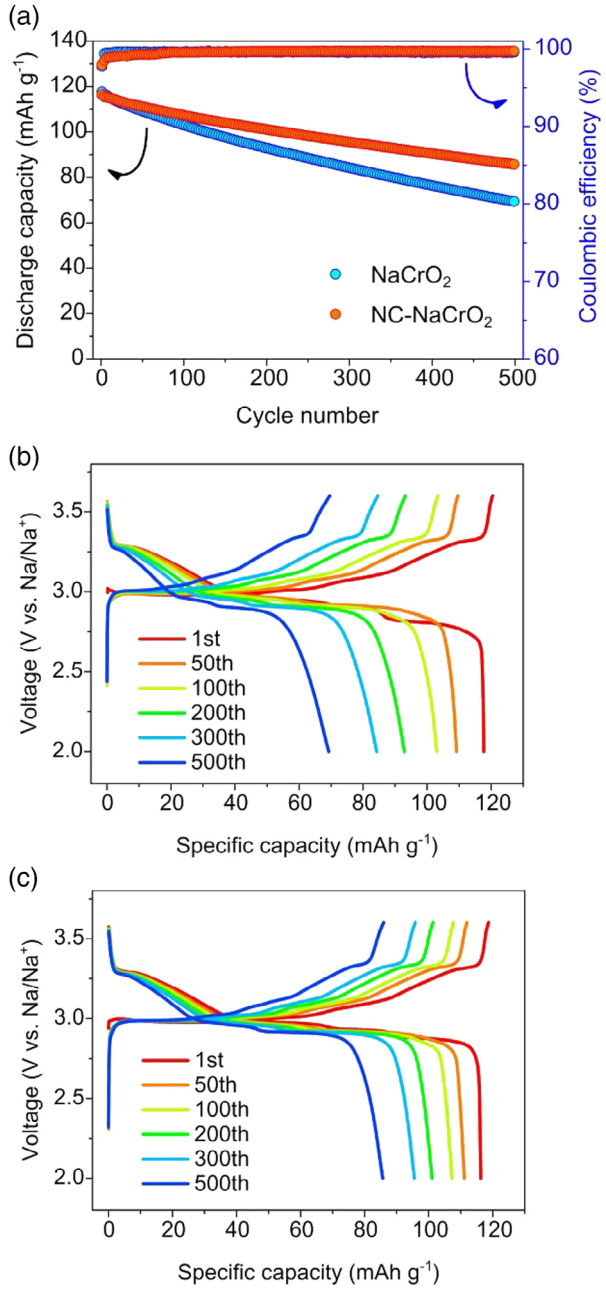

Figure 4. Electrochemical cycling performances of $Na/NaCrO_2$ and $Na/NC–NaCrO_2$ cells during 500 cycles. (a) Specific capacities and Coulombic efficiencies of each sample as a function of cycle number. Galvanostatic charge/discharge curves of (b) $Na/NaCrO_2$ and (c) $Na/NC–NaCrO_2$ cells. Tests were carried out at 100 mA/g between 2 and 3.6 V *vs.* Na/Na^+.

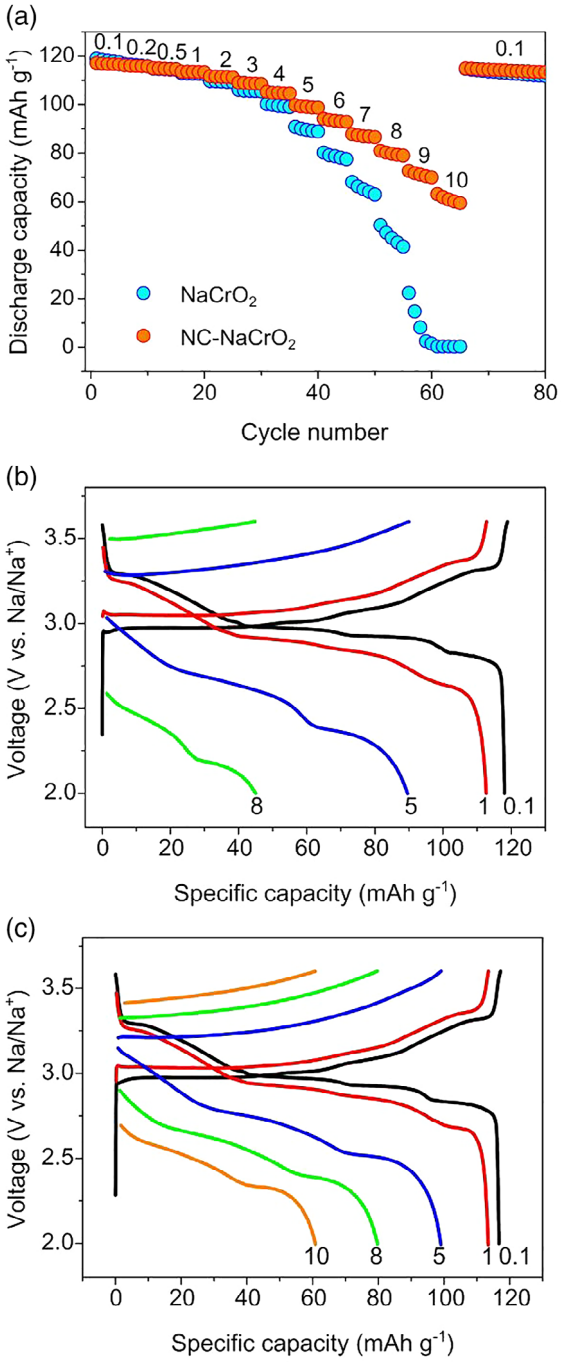

Figure 5. (a) Rate performance of the $Na/NaCrO_2$ and $Na/NC–NaCrO_2$ cells. Charge/discharge curves at different current densities for (b) $Na/NaCrO_2$ and (c) $Na/NC–NaCrO_2$ cells. The numbers in (a)–(c) indicate the magnitude of the current density applied to the cell in a g^{-1}.

decrease in capacity was more pronounced at the biphasic region (approximately 3 V *vs.* Na/Na^+) than at the higher voltage region (above 3 V *vs.* $Na/Na^{+)}$. The major cause of this capacity decay is the O3–P3 transition.[14] Nonetheless, the addition of carbon at the surface of $NC–NaCrO_2$ particles notably enhanced the capacity retention of the material, as carbon acts as a protective layer on the $NaCrO_2$ surface and prevents side reactions with the electrolyte or dissolution of metal at the material surface.[16,17]

To verify their rate capabilities, galvanostatic charge/discharge tests were conducted with current densities of 0.1 (0.83C) to 10 A/g (83C) on both $Na/NaCrO_2$ and $Na/NC–NaCrO_2$ cells (Figure 5(a)). Current densities were equally applied for both charging and discharging. From 0.1 (0.83C) to 3 A/g (25C), both samples exhibited good capacity retentions. For current densities over 4 A/g

(33C), the presence of CW-derived carbon led to noticeable differences in capacity retention between the two cells. At a current density of 5 A/g, $NaCrO_2$ and NC–$NaCrO_2$ exhibited discharge capacities of 89.6 and 99.0 mAh/g, respectively. The charge/discharge curves for the $NaCrO_2$ and NC–$NaCrO_2$ cells confirmed that the differences in polarization and onset potential sharply increased at current densities greater than 8 A/g (Figure 5(b) and (c)). At 9 A/g, carbon-free $NaCrO_2$ suffered from a severe discharge capacity reduction, and almost no discharge capacity was exhibited owing to its limited rate capability, as shown in Figure 5(a). In contrast, NC–$NaCrO_2$ showed no shutdown, even at 10 A/g, and maintained a discharge capacity of approximately 60 mAh/g during rapid charging and discharging. This means that NC–$NaCrO_2$ can exhibit approximately 50% of its total practical capacity with a 43 s charge. After rapid charge/discharge cycles, a low current density of 0.1 A/g was applied again, and both samples recovered discharge capacities close to their initial values. Thus, the difference in discharge capacities at very high current densities was attributed to differences in kinetic properties between the samples. The nitrogen-doped carbon layer from CW at the $NaCrO_2$ surface facilitates electron transfer from a current collector to $NaCrO_2$ particles owing to its high electrical conductivity.[21] This allows for Na^+ insertion and extraction in $NaCrO_2$, even at extremely high current densities.

The improved electrical conductivity of the sample was also evidenced by the EIS results. Figure 6 shows the Nyquist plots for the Na/$NaCrO_2$ and Na/NC–$NaCrO_2$ cells at 2 V *vs.* Na/Na^+ after the first charge and discharge cycles. Both samples exhibited the same behavior, with a semicircle in the high-frequency region and a straight line in the low-frequency region. The semicircle and straight line reflect the charge-transfer resistance (R_{ct}) and Warburg impedance (W, solid-state Na^+ diffusion in bulk), respectively. A comparison of the two Nyquist plots shows that the semicircle of NC–$NaCrO_2$ was smaller than that of bare $NaCrO_2$, indicating that NC–$NaCrO_2$ has a lower charge transfer resistance. Thus, the CW-derived N-doped carbon on the $NaCrO_2$ surface improves the electrical conductivity of $NaCrO_2$, thereby effectively enhancing the rate capability of $NaCrO_2$.

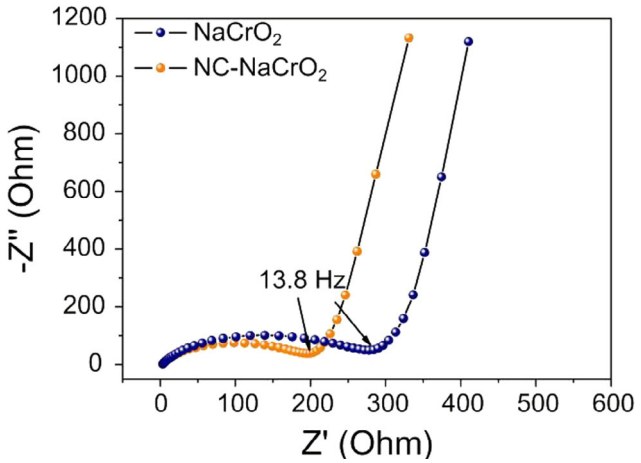

Figure 6. Nyquist plots from EIS data of Na/$NaCrO_2$ and Na/NC–$NaCrO_2$ cells.

Conclusion

In summary, an $NaCrO_2$/CW-derived nitrogen-doped carbon composite was successfully synthesized by an eco-friendly and economic route. N-doped carbon layers were formed on the surface of $NaCrO_2$ particles after mixing of $NaCrO_2$ and CW followed by a short period of heat treatment. When used as a cathode in NIBs, NC–$NaCrO_2$ exhibited a significantly improved electrochemical performance compared to pristine $NaCrO_2$. NC–$NaCrO_2$ showed a 73.7% cycle retention after 500 cycles and an outstanding rate capability in both charge and discharge processes, with an approximate 50% capacity retention even under a current density of 83C (10 A/g). This is owing to the electrical conductivity improvements by the surface N-doped carbon, which was confirmed by EIS results. We believe that this facile synthetic method for NC–$NaCrO_2$ is an approach that can solve the recycling issue of CW and improve the economic feasibility of manufacturing carbon-coated $NaCrO_2$ as a promising NIB cathode material, especially for high-power applications. Furthermore, we believe that this approach can be applied to various electrode materials such as TiO_2, Fe_xO_y, $LiFePO_4$, and so on using different biomass materials.

Acknowledgments. This research was supported by the Institute of Basic Science (IBS) in Korea (IBS-R006-A2) and the 2018 World-Class Professor Program at the Faculty of Engineering Universitas Indonesia funded by the Ministry of Research, Technology and Higher Education, Republic of Indonesia. C. Hudaya acknowledged the support of USAID through Sustainable Higher Education Research Alliances (SHERA) Project for Universitas Indonesia's SMART CITY Center for Collaborative Research.

Supporting Information. Additional supporting information is available in the online version of this article.

References

1. M. Armand, J.-M. Tarascon, *Nature* **2008**, *451*, 652.
2. A. Yoshino, *Angew. Chem. Int. Ed.* **2012**, *51*, 5798.
3. G. E. Blomgren, *J. Electrochem. Soc.* **2017**, *164*, A5019.
4. J.-M. Tarascon, *Nat. Chem.* **2010**, *2*, 510.
5. C. Vaalma, D. Buchholz, M. Weil, S. Passerini, *Nat. Rev. Mater.* **2018**, *3*, 18013.
6. Y.-G. Chun, W.-J. Lee, M. Lee, S.-M. Paek, *Bull. Kor. Chem. Soc.* **2018**, *39*, 665.
7. J.-Y. Hwang, S.-T. Myung, Y.-K. Sun, *Chem. Soc. Rev.* **2017**, *46*, 3529.
8. N. Yabuuchi, K. Kubota, M. Dahbi, S. Komaba, *Chem. Rev.* **2014**, *114*, 11636.

9. M. H. Han, E. Gonzalo, G. Singh, T. Rojo, *Energy Environ. Sci.* **2015**, *8*, 81.
10. N. Ortiz-Vitoriano, N. E. Drewett, E. Gonzalo, T. Rojo, *Energy Environ. Sci.* **2017**, *10*, 1051.
11. P.-F. Wang, Y. You, Y.-X. Yin, Y.-G. Guo, *Adv. Energy Mater.* **2018**, *8*, 1701912.
12. S. Komaba, C. Takei, T. Nakayama, A. Ogata, N. Yabuuchi, *Electrochem. Commun.* **2010**, *12*, 355.
13. S.-H. Bo, X. Li, A. J. Toumar, G. Ceder, *Chem. Mater.* **2016**, *28*, 1419.
14. K. Kubota, I. Ikeuchi, T. Nakayama, C. Takei, N. Yabuuchi, H. Shiiba, M. Nakayama, S. Komaba, *J. Phys. Chem. C* **2015**, *119*, 166.
15. X. Xia, J. R. Dahn, *Electrochem. Solid-State Lett.* **2012**, *15*, A1.
16. J.-J. Ding, Y.-N. Zhou, Q. Sun, Z.-W. Fu, *Electrochem. Commun.* **2012**, *22*, 85.
17. C.-Y. Yu, J.-S. Park, H.-G. Jung, K.-Y. Chung, D. Aurbach, Y.-K. Sun, S.-T. Myung, *Energy Environ. Sci.* **2015**, *8*, 2019.
18. A. Zuorro, R. Lavecchia, *J. Clean. Prod.* **2012**, *34*, 49.
19. S. K. Ramasahayam, A. L. Clark, Z. Hicks, T. Viswanathan, *Electrochim. Acta* **2015**, *168*, 414.
20. D. Y. Chung, Y. J. Son, J. M. Yoo, J. S. Kang, C.-Y. Ahn, S. Park, Y.-E. Sung, *ACS Appl. Mater. Interfaces* **2017**, *9*, 41303.
21. M. Inagaki, M. Toyoda, Y. Soneda, T. Morishita, *Carbon* **2018**, *132*, 104.

